Noname manuscript No.
(will be inserted by the editor)

Color Image Segmentation Using Fuzzy C-Regression Model

Min Chen · Simone A. Ludwig

Received: date / Accepted: date

Abstract Image segmentation is one important process in image analysis and computer vision, and is a valuable tool that can be applied in fields of image processing, health care, remote sensing, and traffic image detection. Given the lack of prior knowledge, unsupervised learning techniques like clustering have been largely adopted. Fuzzy clustering has been widely studied and successfully applied in image segmentation. In situations such as limited spatial resolution, poor contrast, overlapping intensities, noise and intensity inhomogeneities, fuzzy clustering can retain much more information than the hard clustering technique. Most fuzzy clustering algorithms have originated from Fuzzy C-Means (FCM) and have been successfully applied in image segmentation. However, the cluster prototype of the FCM method is hyper-spherical or hyper-ellipsoidal. FCM may not provide the accurate partition in situations where data consists of arbitrary shapes. Therefore, a Fuzzy C-Regression Model (FCRM) has been proposed whose prototype is hyper-planed and can either be linear or nonlinear allowing for better cluster partitioning. Thus, this paper implements FCRM and applies the algorithm to color segmentation. The results show that FCRM obtains more accurate results compared to other fuzzy clustering algorithms.

Keywords Color image segmentation · fuzzy c-regression

1 Introduction

Image segmentation [1, 2] is a necessary first process in image analysis and computer vision by correctly classifying the pixels of an image in decision-oriented

Min Chen and Simone A. Ludwig
Department of Computer Science
North Dakota State University
Fargo, ND, USA
E-mail: {min.chen,simone.ludwig}@ndsu.edu

applications. The essential goal of image segmentation is to partition an image into uniform and homogeneous attribute regions based on some likeness measure. Due to the variety and complexity of images, image segmentation is still a very challenging research topic. Various techniques have been introduced for object segmentation and feature extraction. Basically, segmentation approaches for images are based on the discontinuity and similarity of image intensity values [3]. Discontinuity is an approach which partitions an image based on abrupt changes. According to the predefined criteria, the similarity approach is based on partitioning an image into similar regions. Researchers have proposed a variety of techniques to tackle the challenging problem of image segmentation. In general, the image segmentation can be divided into four different categories [4]: thresholding, edge detection, region extraction, and clustering.

Thresholding [5] is one of the most popular approaches for image segmentation because of its simplicity. Image thresholding partitions an image based on gray levels or intensity values of the pixels. The objective of thresholding is to generate a binary representation of the image and classify each pixel into two categories, "dark" or "light". The challenge of thresholding is to find a correct gray level threshold, which can partition an image into a foreground and background.

Edge Detection [6] is one of the most frequently used techniques in image segmentation. The image edges are detected and grouped into contours or surfaces to represent the boundaries of the objects. Edge detection aims to segment an image by finding and placing sharp discontinuities in gray level images. A very large amount of edge detection techniques are available. Each technique is designed to find certain types of edges.

Region extraction techniques [7] divide the entire image into sub-regions based on some criteria. These approaches make use of similarity in intensity, color, and texture to determine the partitioning of an image. Basically, there are two types of region-based methods [8]. One is a region growing approach, which starts with a set of seed points and the regions grow by appending the neighboring pixels around the seed points with similar properties. The major challenges of this approach include how to select appropriate seed points and how to select suitable criteria during the growing process.

Markov Random Field-based (MRF) techniques [9] have recently been applied in image segmentation. The technique is based on the assumption that the true image can be viewed as a realization of a Markov random field with a distribution that can capture the spatial context of a scene [10]. The segmentation problem is an optimization problem that maximizes the marginal probabilities or posterior marginals by the given prior distribution of the true image and the observed noisy image. However, the MRF approaches are quite computationally expensive, and they require fairly accurate knowledge of the ground truth of the image.

Clustering is a process that can classify the objects or patterns into a predefined number of clusters such that the objects within a cluster have similar properties. In general, clustering methods can be divided into hierarchical and

partitional approaches [11]. Hierarchical algorithms produce a nested series of partitions while partitional algorithms produce only one partition. Due to the fact that construction of a dendrogram is computationally prohibitive, partitional algorithms have gained more attention in image segmentation. Partitional algorithms include two main clustering strategies [12]: the hard clustering scheme and the fuzzy clustering scheme. The conventional hard clustering methods classify each object to only one cluster. As a consequence, the results are crisp. On the other hand, fuzzy clustering allows the objects to belong to two or more clusters with varying degrees of membership. Fuzzy clustering plays a significant role in various problems such as feature analysis, systems identification, and classification design [13]. Fuzzy clustering is more realistic than hard clustering due to the ability of handling impreciseness, uncertainty, and vagueness for real-world problems.

Fuzzy clustering has been widely studied and successfully applied in image segmentation. In situations such as limited spatial resolution, poor contrast, overlapping intensities, noise and intensity inhomogeneities, fuzzy clustering can retain much more information than the hard clustering technique. Among the fuzzy clustering methods, Fuzzy C-Means (FCM) [14] is one of the most popular methods. FCM classifies an image into different clusters using an iterative method. The image is represented in various feature spaces, and FCM groups similar data points that are dependent on the distance of the pixels to the centroids in the feature domain.

The Fuzzy C-Regression Model (FCRM) was introduced by Hathaway and Bezdek [15, 16]. Due to their excellent capability of describing complex systems in a human intuitive way, FCRM is capable of handling perceptual uncertainties and describing nonlinear system. FCRM, which can be viewed as an extension of FCM, divides the data set into a group of different regression models. Unlike FCM, the clustering prototype of FCRM is a hyper-plane while FCM is hyper-spherical.

However, because of the complexity of image segmentation and given that only partial prior knowledge is provided, the segmentation result would be poor if a supervised method was adopted. Thus, the unsupervised method is a better choice to solve such a problem. Although fuzzy theory has been employed in image segmentation, the application of FCRM to color images has been limited. In this paper, we explore the applicability and soundness of FCRM in color image segmentation. Although FCM can partition the fuzzy space efficiently, it does not take linearity of the divided data into consideration. In contrast, the FCRM clustering algorithm with hyperplane-shaped cluster prototypes has much more explanatory power, especially due to its multivariate nature.

The remainder of the paper is organized as follows. Section 2 lists the related work regarding fuzzy image partitioning. Section 3 describes the fuzzy c-regression model and the proposed approach applied to color image segmentation. Experimental results are presented in Section 4, and conclusions are drawn in Section 5.

2 Related Work

Related work with regards to the use of fuzzy theory in image segmentation include rule-based methods, fuzzy-geometrical methods, information theoretical methods, Type II thresholding methods, and fuzzy clustering methods [17].

Past research related to rule-based methods use fuzzy rules to determine a threshold in image segmentation. Images are considered as typical nonstationary signals. Fuzzy rule-based image processing techniques are applied to noise removal and edge extraction. A novel approach for enhancing the results of fuzzy clustering for solving image segmentation problems is introduced in [18]. A Sugeno-type rule-based system is developed to interact with the clustering result obtained by the FCM algorithm. In [19], an approach which combines an associative restoration algorithm with a fuzzy image enhancement technique is presented and is applied in electronic portal images in radiotherapy. However, fuzzy rule based segmentation is sensitive to both the structure of the membership functions and parameter value selections. Thus, a generic fuzzy rule-based segmentation technique that tries to solve the problem of manual selection of the parameters of the fuzzy membership is introduced in [20]. This proposed technique is application-independent and incorporates spatial relationships between pixels. Fuzzy Rules for Image Segmentation incorporating Texture features (FRIST) is proposed in [21]. The fractal dimension and contrast features of texture are incorporated in FRIST by considering image domain specific information.

Fuzzy-geometrical methods [22], which focus on local image information, minimize or maximize fuzzy geometrical measures, such as compactness [23]. In [24], a new approach to multidimensional data clustering is described. The approach developed a "Radar" diagram shape matching methodology to accomplish the fuzzy geometric features technique for man-machine expert systems. A new quantitative index for image segmentation using the concept of homogeneity within regions is defined in [26]. The proposed index shows that the fuzzy geometry based thresholding algorithms produced a single stable threshold for a wide range of membership variations. A semi-supervised FCM technique called GG-FCM is used to add geometrical information during clustering [25]. The approach is not only based on spectral information obtained by FCM, but also takes into consideration the geometrical relationship between neighboring pixels.

Related work on information theoretical methods uses measurements such as fuzzy entropy, index of fuzziness, and fuzzy divergence to minimize or maximize fuzzy information. In [27], a new measure called divergence between two fuzzy sets is introduced and a tailored version of the probability measure of a fuzzy event is also used for image segmentation. A complete method can be viewed as a weighted moving average technique, greyness ambiguity being the weights is introduced in [28]. An image thresholding approach based on the index of nonfuzziness maximization of the 2-D grayscale histogram is introduced in [29], and has shown that the approach is more robust when applied to noisy images.

Type II thresholding methods interpret image information as Type II. In [30], an evolving fuzzy classifier approach that is able to adapt and evolve at an on-line machine vision system is introduced. In [31], a new modified thresholding measures for MRI brain images using type-1 and type-2 fuzzy sets is presented. An Interval Type 2 (IT2) fuzzy entropy based approach is used to compute optimum thresholds for multistage gray scale image segmentation in [32]. An automatic leukocyte segmentation using intuitionistic fuzzy and interval Type II fuzzy set theory in pathological blood cell images is presented in [33]. The use of intuitionistic fuzzy set and interval Type II fuzzy set can consider more uncertainities and different types of uncertainty as compared to basic fuzzy set theory.

Fuzzy clustering methods classify all image pixels into different segments. Up to now, FCM is one of the most commonly used methods in image segmentation, and there have been many variants of fuzzy clustering algorithms that originated from FCM. A modified fuzzy c-means clustering algorithm for MR brain image segmentation is introduced in [34]. The proposed algorithm extracts a scalar feature value from the neighborhood of each pixel. It converges faster than standard FCM in the case of mixed noise. An improved FCM algorithm for image segmentation, which introduces a tradeoff weighted fuzzy factor and a kernel metric is introduced in [35]. The proposed algorithm using a tradeoff weighted fuzzy factor can accurately estimate the damping extent of neighboring pixels. FCM is sensitive to noise in the image since it ignores the spatial information contained in the pixels. A novel fuzzy clustering algorithm with non-local adaptive spatial constraints is presented in [36]. The approach uses an adaptive spatial parameter for each pixel to guide the noisy image segmentation process. Reference [37] proposes the weighted image patch-based FCM algorithm for image segmentation. The algorithm improves its robustness to noise by incorporating local spatial information embedded within the segmentation process. In color image segmentation, it is difficult to analyze the image on all of its colors. Soft computing techniques namely FCM, possibilistic fuzzy c-means, and competitive neural networks have been used to group likely colors [38]. A novel initialization scheme to determine the cluster number and obtain the initial cluster centers for the FCM algorithm to segment color images is introduced in [39]. The initialization scheme called hierarchical approach is proposed to integrate the splitting and merging techniques to obtain the initialization condition for FCM. The proposed algorithm can obtain the reasonable cluster number for any kind of color images. An Adaptive Neuro-Fuzzy Color Image Segmentation (ANFCIS) approach is presented in [40]. The proposed algorithm performs color image segmentation using multilevel thresholding, which consists of a multilayer perceptron-like network.

Most fuzzy clustering algorithms have originated from FCM, and have been successfully applied in image segmentation. However, the cluster prototype of the FCM method is either hyper-spherical or hyper-ellipsoidal. FCM may not provide the accurate partition in situations where data consists of arbitrary shapes. On the other hand, the prototype of the FCRM method is hyper-planed

and can either be linear or nonlinear. Thus, this paper implements FCRM and applies it to color segmentation. The results show that FCRM obtains more accurate results compared to other fuzzy clustering algorithms. Furthermore, besides presenting FCRM's competitiveness with respect to the other fuzzy clustering algorithms, FCRM's practical value is demonstrated when applied to the task of color image segmentation.

3 Proposed Approach

This section first describes the color space that is used for the proposed color segmentation approach, followed by the proposed fuzzy c-regression model clustering approach, and the cluster validation techniques used for the evaluation of the approach.

3.1 CIE-L*A*B* Color Space

Color space is a way of representing color information based on certain criteria. Color perceived by human-beings combines primary colors which are R (red), G (green), and B (blue). By using either linear or nonlinear transformations, other kind of color representations or spaces can be derived from the R, G, and B representation [41]. Color spaces like RGB, HSV (Hue-Saturation-Value) [42], and CIE-L*A*B* [43] have been successfully applied in color image segmentation. In this paper, the CIE-L*A*B* color space is selected and explored in color image segmentation. CIE-L*A*B* is a color-opponent space with dimensions L, A, and B. L denotes as lightness, and A and B are the color-opponent dimensions. The CIE-L*A*B* color space includes all perceivable colors and it is device independent, which means that the colors are independent of the device they are displayed on. Specifically, L with a range between 0 and 100 represents the lightness; 0 represents the darkest black, while 100 represents the brightest white. The red-green opponent colors are represented by the A axis. The yellow-blue opponent colors are represented by the B axis. Both A and B have negative and positive values. Negative values of A represent green colors while positive values of A represent red colors. Similarly, negative values of B represent yellow colors, and positive values of B represent blue colors. The range of A and B can be either ± 100 or ± 128 depending on the specific implementation.

3.2 Fuzzy C-Regression Model Clustering

The fuzzy c-regression model clustering algorithm has become popular the past few years since the resulting model can explain and describe complex systems in a human intuitive way. Takagi and Sugeno [44] introduced the well-known T-S fuzzy model to describe a complicated nonlinear system. A T-S fuzzy

model consists of a set of fuzzy rules, each describing a local input-output relation as follows.

Rule i: IF x_1 is A_1^i and ... and x_M is A_M^i THEN

$$y_i = \theta_i^0 + \theta_i^1 x_1 + ... + \theta_i^M x_M \tag{1}$$

where $X = [x_1, ..., x_M]$ is the system input, M is the dimension of input vector, $i = 1, ..., c$ is the number of fuzzy rules, y_i is the i^{th} output, θ_i^M is the consequent parameter of the i^{th} output.

Fuzzy clustering as one of the soft computing techniques can allow the data points to belong to more than one cluster. Fuzzy clustering has been successfully applied in data analysis, pattern recognition, and image segmentation [38]. The shell clustering algorithms such as FCM have been largely applied in image segmentation. The shell clustering algorithms detect the special geometrical shapes like circles, rectangles, hyperbolas, and ellipses using the Euclidean distance measure [38]. Unlike the shell clustering algorithms, the Fuzzy C-Regression Model (FCRM) [15,16], which was introduced by Hathaway and Bezdek in 1993, assumes that the data is drawn from c different models instead of one single model. The c different models represent c hyper-plane-shape clusters. The FCRM clustering algorithm is an affine T-S model with a linear prototype.

Let $S = (x(k), y_k), k = 1, ..., N$ be a set of input-output sample data pairs, where N is the number of patterns, $x_k = [x_1, x_2, ..., x_M] \subset R^n$ is the k^{th} input data vector, M is the number of input variables, y is output vector, y_k is the k^{th} desired output for x_k, and $\theta_i = [b_i^0, b_i^1, ..., b_i^M]$ is the parameter vector of the corresponding local linear model. Assume that the data pairs in S are drawn from c different fuzzy models. The i^{th} hyper-plane-shaped cluster of the k^{th} input can be denoted as:

$$\begin{aligned} y_k^i &= b_i^0 + b_i^1 x_{k1} + ... + b_i^M x_{kM} \\ &= [x_k, 1] \cdot \theta_i^T, i = 1, ..., c \end{aligned} \tag{2}$$

The cost function of the FCRM clustering algorithm is defined as:

$$J(S; U, \theta) = \sum_{k=1}^{N} \sum_{i=1}^{c} (\mu_{ik}^m) E_{ik}^2(\theta_i) \tag{3}$$

where the distance $E_{ik}(\theta_i)$ is defined as

$$E_{ik}(\theta_i) = |y_k - [x_k 1] \cdot \theta_i^T| \tag{4}$$

m is fuzzy weighted exponent and μ_{ik} is the membership degree of x_k to the i^{th} hyper-plane-shaped cluster. The membership values μ_{ik} have to satisfy the following constraints:

$$\mu_{ik} \in [01], i = 1, 2, .., c; \; k = 1, 2, ...N \tag{5}$$

$$\sum_{i=1}^{c} \mu_{ik} = 1, k = 1, 2, ..., N \tag{6}$$

The fuzzy c-regression model clustering algorithm is summarized as follows [15,16]. Given data S, set $m > 1$ and specify the regression models, choose an error measure and a termination threshold $\epsilon > 0$, and initialize $U^{(0)}$ randomly.

1. Repeat for $l = 1, 2, ...$
2. Calculate the c model parameters $\theta_i^{(l)}$, which globally minimizes the cost function
3. Update $U^{(l)}$ with $E_{ik}(\theta_i^{(l)})$ to satisfy

$$U_{ik}^{(l)} = \begin{cases} [\sum_{j=1}^{c} (\frac{E_{ik}}{E_{jk}})^{\frac{2}{m-1}}]^{-1}, & \text{if } E_{ik} > 0 \text{ for } 1 \leq i \leq c. \\ 0, & \text{otherwise} \end{cases} \tag{7}$$

4. Until $||U^{(l)} - U^{(l-1)}|| \leq \epsilon$, then stop; otherwise, $l = l + 1$ and return to Step 1

In this paper, the FCRM clustering algorithm is applied to color image segmentation. The procedures of the proposed approach using FCRM in color image segmentation can be summarized into four phases: image pre-processing, FCRM clustering, image reconstruction, and evaluation.

Image pre-processing: the images are converted from the RGB color space to the CIE-L*A*B* color space during this phase. The *A and *B values, which are extracted from the RGB color space, serve as the color markers in the A*B* space.

FCRM clustering: the A*B* space image data is given, and the number of clusters is fixed during this phase. A FCRM clustering algorithm is used to partition the given data into a fixed number of clusters.

Image reconstruction: the cluster results from the FCRM clustering step is used to reconstruct the image in grayscale-level during this phase.

Evaluation: the performance of the cluster results is evaluated using the results from the FCRM clustering process. The performance of the proposed algorithm is evaluated with three validity indices (explained in the following section). In addition, two other measures commonly used to access FCRM are calculated during this phase.

3.3 Clustering Validation Techniques

The aim of clustering validation is to evaluate the clustering results by finding the best partition that fits the underlying data best. Thus, cluster validity is used to quantitatively evaluate the results of clustering algorithms. Compactness and separation are two widely considered criteria for measuring the quality of the partitioning of a data set into different numbers of clusters. Conventional approaches use an iterative approach by choosing different input values, and they select the best validity measure to determine the "optimum" number of clusters. A list of validity indices for fuzzy clustering is listed below.

3.3.1 Partition Coefficient (PC) Index

The Partition Coefficient (PC) is defined as [15]:

$$PC = \frac{1}{n}\sum_{i=1}^{n}\sum_{j=1}^{c} u_{ij}^2 \tag{8}$$

PC obtains its maximum value when the cluster structure is optimal.

3.3.2 Partition Entropy (PE) Index

The Partition Entropy (PE) was defined as [48]:

$$PE = -\frac{1}{n}\sum_{i=1}^{n}\sum_{j=1}^{c} u_{ij} log_b(u_{ij}) \tag{9}$$

where b is the logarithmic base. PE achieves its minimum value when the cluster structure is optimal.

3.3.3 Modified Partition Coefficient (MPC) Index

Modification of the PC index, which can reduce the monotonic tendency, was proposed by Dave in 1996 [49].

$$MPC = 1 - \frac{c}{c-1}(1 - PC) \tag{10}$$

where c is the number of clusters. An optimal cluster number is found by maximizing MPC to produce the best clustering performance for a data set.

4 Experiments and Results

This section describes the experimental setup used, and the results obtained by the experiments conducted. In particular, a comparison of the cluster performance in the *A*B space is conducted applying FCM, GK (Gustafson-Kessel), and the proposed FCRM approach. Then, the different validity indices are compared with, followed by a comparison of the mean square error and the peak-signal-to-noise ratio. The last subsection shows the segmentation results.

4.1 Experimental Setup

The experiments are implemented and evaluated on an ASUS desktop (Intel(R) Dual Core I3 CPU @3.07 GHz, 3.07 GHz) Matlab Version 7.13. In order to evaluate the performance of the proposed method, the algorithm has been tested using 15 images from UC Berkeley repository [45] for color image segmentation. In addition, the two other fuzzy clustering algorithms, FCM and Gustafson-Kessel (GK), have been used to compare FCRM with. Table 1 lists the required parameters using FCRM.

Table 1: Parameters and their values of the proposed FCRM algorithm

Parameter	Value
Maximum number of cluster	10
Maximum iteration	50
Image data	IMG1-15
Fuzzification coefficient (m)	2

4.2 Experimental Study

*4.2.1 Comparison of cluster performance in *A*B space*

The cluster performance of IMG1 (all fifteen images are denoted by their number) with $c = 3$ is displayed in Figure 1. The figure on the left is the original image. The remaining three figures show the cluster centers in CIE-L*A*B* color space using FCM, GK, and FCRM, respectively. The three hyper-sephecial centers obtained by FCM and GK, and the three hyper-plane-shaped clusters obtained by FCRM are listed in Table 2.

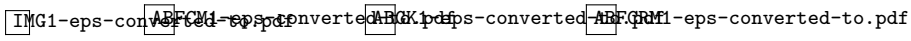

Fig. 1: Original image, FCM, GK, and FCRM with c=3 in *a*b color space

Table 2: FCM, GK, and FCRM using three different indices (PC, PE and MPC)

	FCM	**GK**	**FCRM**
Cluster 1	(151.73, 168.49)	(122.26, 146.33)	$y_1 = 0.3297 \times (x - 80) + 171.2430$
Cluster 2	(103.24, 175.97)	(114.69, 132.16)	$y_2 = 1.1788 \times (x - 101.34) + 110$
Cluster 3	(118.33, 144.69)	(135.42, 158.93)	$y_3 = 0.4578 \times (x - 80) + 142.315$

As shown in Figure 1, the proposed FCRM partitions the image into 3 hyper-planed clusters, while FCM and GK group the image into hyper-spherical clusters, respectively. The FCRM method provides better results of the constructed fuzzy model as compared to FCM and GK.

4.2.2 Comparison using different validity indices

Table 3 lists the cluster performance of FCM, GK, and FCRM using validity index PC, PE, and MPC, respectively. As shown in the table, the values in bold denote the best values obtained from the three different validity indices. In most cases, FCRM has the better performance compared to FCM and GK.

Table 3: FCM, GK, and FCRM using three different indices (PC, PE and MPC)

	PC			**PE**			**MPC**		
	FCM	**GK**	**FCRM**	**FCM**	**GK**	**FCRM**	**FCM**	**GK**	**FCRM**
IMG1	0.77	0.77	**0.81**	0.44	0.44	**0.35**	0.65	0.65	**0.71**
IMG2	0.79	**0.82**	0.78	0.38	**0.34**	0.39	0.68	**0.73**	0.68
IMG3	0.72	0.69	**0.78**	0.50	0.55	**0.40**	0.58	0.53	**0.67**
IMG4	0.68	0.70	**0.80**	0.57	0.53	**0.35**	0.51	0.54	**0.70**
IMG5	0.67	0.68	**0.80**	0.58	0.56	**0.36**	0.51	0.52	**0.70**
IMG6	0.66	**0.83**	0.81	0.56	**0.32**	0.35	0.50	**0.75**	0.71
IMG7	**0.88**	0.83	**0.88**	0.23	0.30	**0.22**	0.81	0.75	**0.83**
IMG8	0.77	0.77	**0.82**	0.42	0.41	**0.33**	0.66	0.65	**0.73**
IMG9	0.74	0.75	**0.79**	0.46	0.45	**0.38**	0.61	0.63	**0.68**
IMG10	0.69	0.72	**0.78**	0.55	0.48	**0.39**	0.54	0.58	**0.67**
IMG11	0.75	**0.77**	**0.77**	0.46	**0.40**	0.41	0.62	**0.66**	**0.66**
IMG12	0.75	0.74	**0.80**	0.46	0.46	**0.37**	0.62	0.61	**0.69**
IMG13	0.75	0.74	**0.83**	0.45	0.47	**0.31**	0.63	0.62	**0.74**
IMG14	0.85	0.84	**0.87**	0.28	0.30	**0.25**	0.77	0.76	**0.80**
IMG15	0.65	0.66	**0.78**	0.62	0.60	**0.40**	0.48	0.48	**0.67**

In addition, the best cluster number of FCM, GK, and FCRM obtained by using PC, PE, and MPC are listed in Table 4. In most cases we can see that the best cluster number is 2 when using PC, PE, and MPC as the validity index.

4.2.3 Comparison with MSE and PSNR

Mean Square Error (MSE) [46] and Peak Signal-to-Noise Ratio (PSNR) [47] are used as the performance indices in fuzzy modeling, which are defined as:

$$MSE = \frac{1}{n}\sum_{k=1}^{n}(y_k - \hat{y}_k)^2 \tag{11}$$

$$PSNR = \frac{10 \times (255 \times 255/MSE)}{log(10)} \tag{12}$$

Table 5, 7, 9 list the MSE of the 15 images using FCM, GK, and FCRM, respectively. Table 6, 8, 10 list the PSNR of the 15 images obtained from FCM, GK, and FCRM, respectively. The results show that FCM, GK and FCRM show the same trend regarding MSE and PSNR. As the number of clusters increase, the values of MSE decrease, and the values of PSNR increase for the 15 tested images. In addition, FCRM has a better performance than FCM and GK both in terms of MSE and PSNR.

Table 4: Best cluster number of FCM, GK and FCRM using PC, PE and MPC

	PC			PE			MPC		
	FCM	**GK**	**FCRM**	**FCM**	**GK**	**FCRM**	**FCM**	**GK**	**FCRM**
IMG1	3	2	3	2	2	2	2	2	2
IMG2	2	2	2	2	2	3	2	2	7
IMG3	2	2	2	2	2	2	2	2	2
IMG4	2	2	2	10	10	10	2	2	10
IMG5	2	2	2	2	2	2	2	2	2
IMG6	2	2	2	3	3	3	2	2	2
IMG7	2	2	2	2	2	2	2	2	2
IMG8	2	2	2	3	2	3	2	2	3
IMG9	2	2	2	2	2	2	2	2	2
IMG10	2	2	5	2	2	2	2	2	2
IMG11	2	2	4	2	2	3	2	2	4
IMG12	2	2	2	2	2	2	2	2	2
IMG13	2	2	5	2	2	3	2	2	3
IMG14	2	2	2	2	2	10	2	2	2
IMG15	2	2	2	2	2	2	2	2	2

4.2.4 Comparison on segmentation results

The cluster results are used to reconstruct the image in grayscale level as shown in Figures 2 and 3 with $c = 3$. As show in the figures, the FCM, GK, and FCRM can segment the images clearly.

5 Conclusion

Most fuzzy clustering algorithms have been successfully applied in image segmentation. However, the disadvantage they have is that the cluster prototype of FCM (Fuzzy C-Means) is either hyper-spherical or hyper-ellipsoidal. Therefore, FCM may not provide accurate partitioning in circumstances where data is better modeled by arbitrary shapes. Thus, a Fuzzy C-Regression Model (FCRM) clustering algorithm has been introduced whose prototype is hyperplaned and can either be linear or nonlinear. The FCRM clustering algorithm and applied it to color image segmentation. FCRM is an affine T-S model, which has been successfully used in non-linear system. Due to the complexity of implementation, FCRM has never been used in color image segmentation and was thus explored in this investigation.

The experiments conducted used 15 images that were taken from the UC Berkeley repository. The FCRM was compared against two comparison algorithms (FCM and GK) for color image segmentation. Three validity indices

Table 5: MSE using FCM with different cluster number

	c=2	**3**	**4**	**5**	**6**	**7**	**8**	**9**	**10**
IMG1	0.59	0.41	0.32	0.26	0.21	0.19	0.16	0.14	0.13
IMG2	0.37	0.26	0.19	0.16	0.13	0.12	0.10	0.09	0.08
IMG3	0.79	0.54	0.40	0.32	0.27	0.23	0.20	0.18	0.16
IMG4	1.05	0.70	0.50	0.42	0.34	0.29	0.26	0.23	0.21
IMG5	0.39	0.27	0.21	0.16	0.14	0.12	0.10	0.09	0.08
IMG6	0.48	0.41	0.33	0.28	0.23	0.20	0.17	0.15	0.14
IMG7	0.41	0.27	0.26	0.25	0.21	0.17	0.16	0.14	0.13
IMG8	0.50	0.34	0.25	0.20	0.17	0.14	0.13	0.11	0.10
IMG9	0.97	0.66	0.50	0.40	0.33	0.29	0.25	0.22	0.20
IMG10	0.99	0.69	0.56	0.46	0.39	0.33	0.29	0.26	0.23
IMG11	0.93	0.62	0.47	0.38	0.31	0.27	0.24	0.21	0.19
IMG12	0.79	0.55	0.43	0.41	0.34	0.30	0.26	0.23	0.21
IMG13	0.64	0.45	0.34	0.27	0.23	0.20	0.17	0.15	0.13
IMG14	0.73	0.49	0.37	0.24	0.19	0.17	0.15	0.13	0.13
IMG15	0.58	0.40	0.30	0.24	0.20	0.18	0.16	0.14	0.13

have been used as well as MSE and PSNR were measured. The images were reconstructed using the grayscale level. The experimental results revealed that FCRM achieves better results in most cases than the other approaches based on the aforementioned measures.

As for future work, FCRM is similar to other fuzzy partition techniques, thus, cluster centroids and the number of clusters should be decided in advance. However, for most unknown environments, the appropriate and exact number of clusters is unknown in practice. A new cluster validity criterion needs to be developed to determine the appropriate number of clusters. In addition, FCRM is very sensitive to the initialization. A good initialization results in good quality image segmentation, while an unsuitable initialization returns poor results. Thus, in future, a new technique for automatically finding the exact number of clusters as well as obtaining good initialization need to be investigated.

References

1. L. G. Shapiro and G. C. Stockman, Computer Vision, pp 279-325, New Jersey, Prentice-Hall, (2002).
2. D. L. Pham, C. Xu, J. L. Prince, Current Methods in Medical Image Segmentation, Annual Review of Biomedical Engineering 2: 315337, (2000).
3. J. Malik, S. Belongie, T. Leung, and J. Shi, Contour and texture analysis for image segmentation. International journal of computer vision, 43(1), 7-27, (2001).
4. S. Krinidis, V. Chatzis, A robust fuzzy local information C-means clustering algorithm. Image Processing, IEEE Transactions on, 19(5), 1328-1337,(2010).

Table 6: PSNR using FCM with different cluster number

	c=2	**3**	**4**	**5**	**6**	**7**	**8**	**9**	**10**
IMG1	19.41	12.79	9.49	7.59	6.31	5.40	4.73	4.20	3.78
IMG2	21.48	14.18	10.60	8.37	7.03	5.96	5.21	4.65	4.14
IMG3	16.74	11.11	8.38	6.70	5.58	4.79	4.19	3.72	3.35
IMG4	14.65	9.76	7.45	5.86	4.95	4.25	3.69	3.29	2.93
IMG5	21.58	14.27	10.63	8.49	7.07	6.06	5.30	4.71	4.24
IMG6	19.77	12.12	8.83	6.98	5.82	4.99	4.36	3.88	3.49
IMG7	20.77	13.83	9.57	7.25	6.05	5.32	4.54	4.03	3.59
IMG8	19.35	12.87	9.65	7.71	6.42	5.51	4.82	4.28	3.83
IMG9	15.52	10.27	7.69	6.14	5.12	4.38	3.83	3.41	3.07
IMG10	14.23	9.76	7.05	5.57	4.64	3.97	3.47	3.08	2.77
IMG11	15.29	10.17	7.62	6.10	5.08	4.35	3.81	3.39	3.05
IMG12	16.38	10.75	7.92	5.87	4.89	4.18	3.64	3.23	2.91
IMG13	17.82	11.61	8.70	6.95	5.79	4.94	4.32	3.84	3.52
IMG14	16.89	11.26	8.45	7.25	6.15	5.18	4.51	4.02	3.57
IMG15	18.60	12.26	9.17	7.29	6.07	5.19	4.53	4.03	3.62

5. M. Sezgin, Survey over image thresholding techniques and quantitative performance evaluation. Journal of Electronic imaging, 13(1), 146-168, (2004).
6. N. Senthilkumaran, R. Rajesh, Edge detection techniques for image segmentation a survey of soft computing approaches, International journal of recent trends in engineering, 1(2),(2009).
7. K. Haris, S. N. Efstratiadis, N. Maglaveras, A. K.Katsaggelos, Hybrid image segmentation using watersheds and fast region merging. Image Processing, IEEE Transactions on, 7(12), 1684-1699, (1998).
8. J. Fan, D. K. Yau, A. K. Elmagarmid, W. G. Aref, Automatic image segmentation by integrating color-edge extraction and seeded region growing. Image Processing, IEEE Transactions on, 10(10), 1454-1466, (2001).
9. T. Kasetkasem, M. K. Arora, P. K. Varshney, Super-resolution land cover mapping using a Markov random field based approach. Remote Sensing of Environment, 96(3), 302-314, (2005).
10. F. Amat, F. Moussavi, L. R. Comolli, G. Elidan, K. H. Downing, M. Horowitz, Markov random field based automatic image alignment for electron tomography. Journal of structural biology, 161(3), 260-275, (2008).
11. Z. Wu, R. Leahy, An optimal graph theoretic approach to data clustering: Theory and its application to image segmentation. Pattern Analysis and Machine Intelligence, IEEE Transactions on, 15(11), 1101-1113, (1993).
12. K. S. Chuang, H. L. Tzeng, S. Chen, J. Wu, T. J. Chen, Fuzzy c-means clustering with spatial information for image segmentation. computerized medical imaging and graphics, 30(1), 9-15, (2006).
13. N. R. Pal, S. K. Pal, A review on image segmentation techniques. Pattern recognition, 26(9), 1277-1294, (1993).
14. J. C. Bezdek, R. Ehrlich, W. Full, FCM: The fuzzy c-means clustering algorithm. Computers Geosciences, 10(2), 191-203, (1984).
15. J. C. Bezdek, Pattern Recognition with Fuzzy Objective Function Algorithms, Plenum Press, New York, NY, (1981).

Table 7: MSE using GK with different cluster number

	c=2	**3**	**4**	**5**	**6**	**7**	**8**	**9**	**10**
IMG1	0.62	0.42	0.31	0.26	0.21	0.18	0.16	0.14	0.13
IMG2	0.37	0.26	0.19	0.16	0.13	0.12	0.10	0.09	0.08
IMG3	0.79	0.54	0.40	0.32	0.27	0.23	0.20	0.18	0.16
IMG4	0.82	0.62	0.51	0.42	0.35	0.30	0.26	0.23	0.21
IMG5	0.39	0.26	0.20	0.16	0.14	0.12	0.10	0.09	0.08
IMG6	0.52	0.52	0.40	0.32	0.26	0.20	0.18	0.15	0.14
IMG7	0.41	0.27	0.29	0.24	0.20	0.17	0.14	0.13	0.12
IMG8	0.49	0.34	0.25	0.20	0.17	0.15	0.13	0.11	0.10
IMG9	0.97	0.66	0.50	0.40	0.34	0.29	0.25	0.22	0.20
IMG10	0.98	0.78	0.58	0.47	0.39	0.33	0.29	0.26	0.23
IMG11	0.92	0.62	0.47	0.38	0.31	0.27	0.24	0.21	0.19
IMG12	0.78	0.62	0.47	0.38	0.35	0.30	0.26	0.23	0.21
IMG13	0.68	0.42	0.34	0.27	0.23	0.20	0.16	0.14	0.14
IMG14	0.73	0.49	0.37	0.29	0.24	0.21	0.18	0.16	0.15
IMG15	0.59	0.40	0.30	0.25	0.21	0.18	0.15	0.14	0.13

16. J. C. Bezdek, J. Keller, R. Krisnapuram, and N. Pal, Fuzzy Models and Algorithms for Pattern Recognition and Image Processing, Vol. 4, Springer, New York, NY, (1999).
17. A. Othman and H. Tizhoosh, Evolving fuzzy image segmentation, in Proc. IEEE Int. Conf. Fuzzy Syst., pp. 16031609, Jun. (2011).
18. Y. A. Tolias, S. M. Panas, On applying spatial constraints in fuzzy image clustering using a fuzzy rule-based system. Signal Processing Letters, IEEE, 5(10), 245-247, (1998).
19. H. Tizhoosh, G. Krell, T. Lilienblum, C. J. Moore, and B. Michaelis, Enhancement and associative restoration of electronic portal images in radiotherapy, Int. J. Med. Inf., vol. 49, no. 2, pp. 157171, (1998).
20. G. Karmakar and L. Dooley, A generic fuzzy rule based image segmentation algorithm, Pattern Recognition Letters, vol. 23, no. 10, pp. 12151227, (2002).
21. , G. Karmakar, L. Dooley, and M. Murshed. Fuzzy rule for image segmentation incorporating texture features. 2002 International Conference on In Image Processing, vol. 1, pp. I-797. IEEE, (2002).
22. S. Pal and A. Rosenfeld, Image enhancement and thresholding by optimization of fuzzy compactness, Pattern Recognit. Lett., pp. 7786, (1988).
23. S. K. Pal and A. Ghosh, Fuzzy geometry in image analysis, Fuzzy Sets Syst., vol. 48, no. 1, pp. 2340, (1992).
24. V. V. Krivsha, S. A. Butenkov, Classification using fuzzy geometric features, 2002 IEEE International Conference on Artificial Intelligence Systems, vol., no., pp.89,91, (2002).
25. J. Noordam, W. van den Broek, and L. Buydens, Geometrically guided fuzzy C-means clustering for multivariate image segmentation, in Proceedings of International Conference on Pattern Recognition (ICPR00), vol. 1, pp. 462465, (2000).
26. S. K. Pal, A. Ghosh, B. U. Shankar, Segmentation of remotely sensed images with fuzzy thresholding, and quantitative evaluation. International Journal of Remote Sensing, 21(11), 2269-2300.
27. N. R. Pal, D. Bhandari, and D. D. Majumder, Fuzzy divergence, probability measure of fuzzy events and image thresholding, Pattern Recognit., vol. 13, pp. 857867, (1992).

Table 8: PSNR using GK with different cluster number

	c=2	**3**	**4**	**5**	**6**	**7**	**8**	**9**	**10**
IMG1	19.15	12.74	9.55	7.59	6.32	5.40	4.73	4.20	3.77
IMG2	21.56	14.16	10.60	8.47	7.05	5.98	5.22	4.65	4.17
IMG3	16.76	11.10	8.32	6.65	5.56	4.78	4.18	3.71	3.33
IMG4	16.22	10.29	7.39	5.86	4.88	4.18	3.71	3.25	2.93
IMG5	21.65	14.35	10.67	8.50	7.07	6.06	5.30	4.71	4.23
IMG6	19.23	11.09	8.30	6.63	5.53	4.93	4.31	3.88	3.49
IMG7	20.79	13.84	9.31	7.34	6.13	5.26	4.73	4.10	3.69
IMG8	19.53	12.85	9.64	7.70	6.42	5.50	4.81	4.28	3.83
IMG9	15.55	10.31	7.69	6.14	5.11	4.38	3.83	3.40	3.06
IMG10	13.91	9.20	6.96	5.55	4.63	3.96	3.48	3.09	2.78
IMG11	15.36	10.18	7.62	6.10	5.08	4.35	3.81	3.39	3.05
IMG12	16.46	10.19	7.63	6.07	4.84	4.15	3.63	3.23	2.90
IMG13	17.46	11.93	8.71	6.94	5.76	4.94	4.44	3.95	3.47
IMG14	16.90	11.27	8.45	6.76	5.63	4.82	4.22	3.75	3.37
IMG15	18.49	12.22	9.13	7.29	6.06	5.20	4.54	4.03	3.62

28. C. A. Murthy and S. K. Pal, Fuzzy thresholding: Mathematical framework bound functions and weighted moving average technique, Pattern Recognit. Lett., vol. 11, pp. 197206, (1990).
29. Q. Wang, Z. Chi, and R. Zhao, Image thresholding by maximizing the index of nonfuzziness of the 2-D grayscale histogram, Comput. Vis. Imag. Understand., vol. 85, no. 2, pp. 100116, (2002).
30. E. Lughofer, On-line evolving image classifiers and their application to surface inspection, Imag. Vis. Comput., vol. 28, no. 7, pp. 10651079, (2010).
31. R. Rajesh, N. Senthilkumaran, J. Satheeshkumar, B. S. Priya, C. Thilagavathy, and K. Priya, On the type-1 and type-2 fuzziness measures for thresholding MRI brain images, in Proc. IEEE Int. Conf. Fuzzy Syst., pp. 992995, Jun. (2011).
32. D. Neog, M. Raza, and F. Rhee, An interval type 2 fuzzy approach to multilevel image segmentation, in Proc. IEEE Int. Conf. Fuzzy Syst., pp. 11641170, Jun. (2011).
33. T. Chaira, Accurate segmentation of leukocyte in blood cell images using Atanassov's intuitionistic fuzzy and interval Type II fuzzy set theory. Micron, 61, 1-8, (2014).
34. L. Szilagyi, Z. Beny, S. M. Szilagyi, H. S. Adam, MR brain image segmentation using an enhanced fuzzy C-means algorithm. In Proceedings of the 25th annual international conference of the IEEE engineering in medicine and biology society, Vol. 1, pp. 1721, (2003).
35. M. Gong, Y. Liang, J. Shi, W. Ma, J. Ma, Fuzzy c-means clustering with local information and kernel metric for image segmentation. Image Processing, IEEE Transactions on, 22(2), 573-584, (2013).
36. F. Zhao, L. Jiao, H. Liu, X. Gao, A novel fuzzy clustering algorithm with non local adaptive spatial constraint for image segmentation. Signal Processing, 91(4), 988-999, (2011).
37. Z. Ji, Y. Xia, Q. Chen, Q. Sun, D. Xia, D. D. Feng, Fuzzy c-means clustering with weighted image patch for image segmentation. Applied soft computing, 12(6), 1659-1667, (2012).
38. B. Sowmya, B. S. Rani, Colour image segmentation using fuzzy clustering techniques and competitive neural network. Applied Soft Computing, 11(3), 3170-3178, (2011).

Table 9: MSE using FCRM with different cluster number

	c=2	**3**	**4**	**5**	**6**	**7**	**8**	**9**	**10**
IMG1	0.58	0.40	0.31	0.25	0.21	0.18	0.16	0.14	0.13
IMG2	0.37	0.25	0.19	0.16	0.13	0.12	0.10	0.09	0.08
IMG3	0.80	0.54	0.40	0.32	0.27	0.23	0.20	0.18	0.16
IMG4	1.05	0.70	0.52	0.42	0.35	0.30	0.26	0.23	0.21
IMG5	0.39	0.26	0.20	0.16	0.14	0.12	0.10	0.09	0.08
IMG6	0.48	0.44	0.36	0.28	0.24	0.21	0.18	0.16	0.15
IMG7	0.69	0.27	0.30	0.25	0.21	0.19	0.16	0.14	0.13
IMG8	0.50	0.35	0.26	0.20	0.17	0.15	0.13	0.12	0.10
IMG9	0.98	0.66	0.50	0.40	0.33	0.29	0.25	0.22	0.20
IMG10	0.98	0.80	0.60	0.48	0.40	0.34	0.30	0.27	0.24
IMG11	0.93	0.63	0.47	0.38	0.31	0.27	0.24	0.21	0.19
IMG12	0.80	0.61	0.52	0.42	0.35	0.30	0.26	0.23	0.21
IMG13	0.67	0.45	0.33	0.27	0.23	0.19	0.17	0.15	0.14
IMG14	0.73	0.49	0.37	0.29	0.24	0.21	0.18	0.16	0.15
IMG15	0.57	0.40	0.31	0.25	0.21	0.18	0.16	0.14	0.13

39. K. S. Tan, W. H. Lim, N. A. M.Isa, Novel initialization scheme for Fuzzy C-Means algorithm on color image segmentation. Applied Soft Computing, 13(4), 1832-1852, (2013).
40. K. Deshmukh, G. N. Shinde, An adaptive neuro-fuzzy system for color image segmentation. Journal of the Indian Institute of Science, 86(5), 493, (2013).
41. R. S. Hunter, Photoelectric Color-Difference Meter. JOSA 38 (7): 661, Proceedings of the Winter Meeting of the Optical Society of America, July (1948).
42. J. D. Foley, et al. Computer Graphics: Principles and Practice (2nd ed.). Redwood City, CA: Addison-Wesley, (1995).
43. R. S. Hunter, Accuracy, Precision, and Stability of New Photo-electric Color-Difference Meter. JOSA 38 (12): 1094, Proceedings of the Thirty-Third Annual Meeting of the Optical Society of America, December (1948).
44. T. Takagi and M. Sugeno, Fuzzy identification of systems and its applications to modeling and control, IEEE Trans. Syst. Man Cybern., vol. SMC-15, no. 1, pp. 116132, (1985).
45. C. Fowlkes, D. Martin, J. Malik. Local Figure/Ground Cues are Valid for Natural Images, Journal of Vision, 7(8):2, 1-9, (2007).
46. E. L. Lehmann, G. Casella, Theory of Point Estimation (2nd ed.). New York: Springer, (1998).
47. Q. Huynh-Thu, M. Ghanbari, Scope of validity of PSNR in image/video quality assessment, Electronics Letters 44 (13): 800, (2008).
48. J. C. Bezdek, C. Coray, R. Gunderson and J. Watson, Detection and Characterization of Cluster Substructure. II. Linear Structure, Fuzzy c-Varieties and Convex Combinations Thereof, SIAM J. Appl. Math., Vol.40, No.2, pp.358-372, 1981.
49. R. N. Dave, Validating fuzzy partitions obtained through c-shells clustering. Pattern Recognition Letters, 17(6), 613-623, 1996.

Table 10: PSNR using FCRM with different cluster number

	c=2	**3**	**4**	**5**	**6**	**7**	**8**	**9**	**10**
IMG1	19.52	12.86	9.60	7.64	6.37	5.43	4.76	4.22	3.80
IMG2	21.48	14.19	10.57	8.44	6.98	5.97	5.22	4.63	4.15
IMG3	16.69	11.10	8.32	6.67	5.55	4.76	4.16	3.70	3.33
IMG4	14.66	9.78	7.33	5.86	4.88	4.19	3.66	3.25	2.93
IMG5	21.66	14.33	10.70	8.53	7.08	6.06	5.29	4.70	4.23
IMG6	19.85	11.89	8.64	6.91	5.74	4.91	4.28	3.80	3.42
IMG7	17.51	13.84	9.23	7.26	6.05	5.11	4.47	3.98	3.58
IMG8	19.31	12.73	9.54	7.71	6.36	5.45	4.77	4.24	3.81
IMG9	15.49	10.27	7.70	6.14	5.12	4.38	3.84	3.41	3.07
IMG10	15.02	9.15	6.85	5.48	4.56	3.91	3.42	3.04	2.74
IMG11	15.29	10.16	7.62	6.09	5.08	4.35	3.81	3.38	3.05
IMG12	16.32	10.25	7.28	5.81	4.84	4.15	3.63	3.22	2.90
IMG13	17.50	11.63	8.83	7.03	5.79	5.00	4.37	3.88	3.49
IMG14	16.91	11.26	8.44	6.75	5.62	4.82	4.22	3.75	3.37
IMG15	18.62	12.22	9.10	7.25	6.06	5.18	4.53	4.02	3.60

Fig. 2: Original image, grayscale image using FCM, GK, and FCRM are listed, respectively

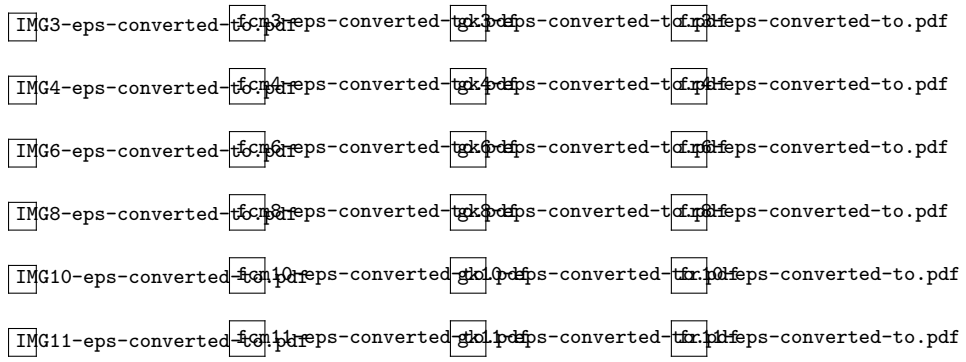

Fig. 3: Original image, grayscale image using FCM, GK, and FCRM are listed, respectively (continued)